



We are Nitinol.™

Finite Element Analysis on Nitinol Medical Applications

Gong, Pelton

Proceedings of the International Conference on Shape Memory and Superelastic
Technologies, SMST-2003

2003

www.nitinol.com

47533 Westinghouse Drive Fremont, California 94539 t 510.683.2000 f 510.683.2001

SMST-2003

Proceedings of the International Conference on

Shape Memory and Superelastic Technologies

5 May to 8 May 2003

Asilomar Conference Center

Pacific Grove, California, USA

Editors

Alan R. Pelton

Tom Duerig



© 2004 by SMST
All rights reserved.

No part of this book may be reproduced, stored in a retrieval system, or transcribed, in any form or by any means—electronic, mechanical, photocopying, recording, or otherwise—without prior permission of the publisher.

Published by:
SMST Society, Inc.
c/o SRI M/S AA287
333 Ravenswood Avenue
Menlo Park, California 94025
USA
Telephone: (650) 879-6476
E-mail: info@smst.org
Website: www.smst.org

Copies of this book may be ordered through the SMST website at www.smst.org or by calling the SMST office at (650) 859-6476, or through ASM International, Customer Service at (440) 338 5151 x5537 or at www.asminternational.org.

Printed and bound in the United States of America

Library of Congress Control Number: 2004102781

Publisher's Cataloging in Publication Data

SMST-2003: proceedings of the international conference on shape memory and superelastic technologies / edited by Alan R. Pelton and Tom Duerig.

xvi; 746 p.; 26 cm

Includes bibliographical references and index.

ISBN 0-9660508-3-5

1. Alloys—Congresses. 2. Alloys—Thermomechanical properties. 3. Shape memory effect. I. Pelton, Alan (Alan R.) II. Duerig, Tom (Thomas W.)

TN690.S675 2004
669'.94—dc20

Production Services by TIPS Technical Publishing, Inc.

FINITE ELEMENT ANALYSIS ON NITINOL MEDICAL APPLICATIONS

Xiao-Yan Gong and Alan R. Pelton

Nitinol Devices & Components, 47533 Westinghouse Drive, Fremont, CA 94539

ABSTRACT

This article presents two applications of nonlinear Finite Element Analysis (FEA). In the first example, FEA predicts the stress-strain response of a superelastic Nitinol device at different austenite finish temperatures (A_f) when tested at 37°C. The second example illustrates the method for evaluating a stent's fatigue performance. The analyses are found to agree well with the theoretical prediction and/or experimental measurement. The focus of this presentation is on the use of FEA as a predictive design tool for fast prototyping of Nitinol medical devices.

KEYWORDS

NiTi, Finite Element Analysis, Medical Application, Stent, Minimally Invasive Surgery

INTRODUCTION

Nitinol's biocompatibility has made it a great material for many medical applications such as dentures, orthodontic arch wires, needles, guide wires, heart valve instruments, self-expanding stents, vena cava filters, minimally invasive surgery instruments, and septal defect occlusion systems, to name a few [1–4]. Many of these devices are implanted into the human body via minimally invasive surgical procedures taking advantage of the unique superelastic behavior of Nitinol. With increasing market demand and competition, a predictive method that can shorten the time and resources from design to production becomes the key in new product development. Traditional beam theory provides reasonable estimations in some applications, but success is limited to small strain [5]. Nonlinear Finite Element Analysis (FEA), which is capable of not only dealing with the complicated geometry, but also modeling the nonlinear material response, becomes more and more important in product design.

The superelastic material behavior generates analysis difficulties due to its path-dependence and high nonlinearity. This calls for efficient constitutive modeling because it is inevitable that numerical iteration is necessary during the analysis. Phenomenological approaches are the most suitable solution for the simulation efficiency. Theories based on either the generalized plasticity theory, which focuses on the material response at a given temperature, or a free energy framework, which focuses on the temperature dependencies of the material, or even the micromechanics models have been developed independently in the past decade [6–13]. Based on several of these approaches, ABAQUS West commercialized a User-defined Material (UMAT) subroutine specific to Nitinol based on the generalized plasticity theory [7–9]. Many applications demonstrated that the UMAT is capable of predicting the uniaxial material response at different temperatures, a Nitinol stent's deformation, and Austenite or Martensite composition at any material point in addition to the stress and strain fields [14–15]. Therefore, it is used in the analyses presented in this paper. Recently, comparison of the Abaqus West UMAT and another UMAT by EchoBio has shown that both approaches agree very well with one another and they both predict the experiment results well [16].

This article focuses on analyzing Nitinol's medical applications in minimally invasive surgery. The analyses are divided into two categories. We choose a representative device from each category and discuss the analysis in detail. The first device analyzed is a Nitinol needle/wire locator. The second device is a self-expanding stent. They are chosen with general indications on many other applications as listed in the section below. In both cases, experimental data are used to compare with the analysis results. Theoretical estimations are also provided to further confirm the analysis results.

In the needle/wire locator application, we show that the UMAT is able to predict the uniaxial material response at different austenite finish temperature (A_f) by comparing with the experimental data. This opens doors for the optimization of the A_f to achieve the most suitable design. It also indicates that the material properties at different A_f or application temperatures are predictive. The stress analysis on the device is straightforward since the hook wire is constrained very tightly inside the needle. Furthermore, the peak stress and strain values can be estimated from pure geometry change. Comparison shows that FEA agrees well with the theoretical prediction.

In the stent application, we briefly review the FEA procedures in evaluating a stent's fatigue strains *in vivo*. Our focus is aimed on the FEA results on a fatigue specimen simulating the deformation of stentlike devices, i.e., a diamond-shaped specimen. Fatigue tests on this test specimen are used to set up the strain-life curve that dictates the baseline for fatigue prediction [17]. FEA results on diamond shaped specimen are compared with the load-displacement results collected from the experiment. A theoretical solution based on a piece-wise linear approximation in combination with the fundamental beam theory is generated on the loading portion of the specimen for comparison. Results show good agreement between FEA, theoretical prediction, and the experimental data.

NEEDLE/WIRE LOCATOR

Figure 1 shows the Mitek Homer Mammalok needle/wire locator. It is a two-piece device that consists of a Nitinol wire with a semicircular-shaped hook at one end, which served as a locator to identify the tumor location in the application, and a hollow needle that the wire slides into. The locator is originally withdrawn inside the needle cannula [18]. During the application, the needle is inserted into the breast and adjusted until its tip is verified to be at the site of the tumor. The locator is then advanced and reforms the hook configuration. The position of the hook marks the correct location for the surgeon. If necessary, the locator can be withdrawn into the needle until the correct location is identified.

The design challenge was to have a strong hook so that it can be placed in position tightly, yet was not too hard to withdraw into the needle. One of the possible design options, from a material application point, was to choose the right A_f temperature. Pelton et al. provided details on how to obtain the desired A_f [19]. Pelton et al. later also pointed out that the best way to optimize both A_f and the geometry is to perform FEA without actually making and testing the device [20]. This type of FEA normally involves a curved wire withdrawn into a straight tube. The analysis is very straightforward. One can mesh the wire with solid elements and simplify the needle as a rigid cylinder. Use of symmetry can reduce the model to a half of its actual size. Prescribed displacement condition can be used to pull the wire through the rigid cylinder. The outputs from FEA are the stress and strain fields and the contact pressure between the wire and the needle (rigid surface). The wire diameter is 0.38 mm and the hook radius is 4.8 mm in this study. The maximum tensile and compressive strains are theoretically estimated from the curved beam theory to be approximately 4.1% and -3.8% respectively.

A uniaxial tensile test is necessary to calibrate the UMAT for analysis. For comparison purposes, the tests were performed at 37°C for wires that are processed to have three different A_f temperatures, i.e., -10°C , 14°C and 27°C . We used the highest A_f , i.e., $A_f = 27^\circ\text{C}$, to calibrate the UMAT. We then run a single element test to predict the stress-strain relations for the other two A_f wires. Figure 2 shows the comparison of the FEA prediction and the experimental results of the highest A_f wire. As one can tell, the calibrated material response reproduces the experimental results very well. Figure 3 shows the comparison of the FEA prediction and the experimental results on the lower A_f wires. Again, the results agree, especially well in the range of application interests, i.e., up to 6%.



Figure 1 Mitek Homer Mammalok needle/wire locator.

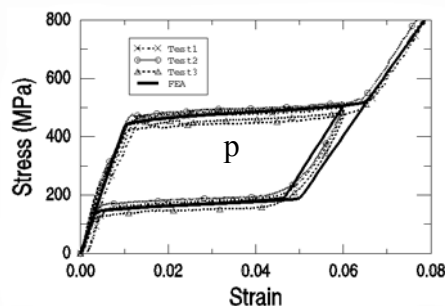


Figure 2 FEA material model calibrated using $A_f = 27^\circ\text{C}$.

Figure 4 shows stress contour on the deformed shape for different A_f wires when they are withdrawn into the needle. Clearly the different A_f wires produce different magnitudes of stress field. The lower the A_f , the higher the stress it produces. Therefore, the lower the A_f , the harder it is to withdraw the wire into the needle. When the strain contours are plotted, there is less difference

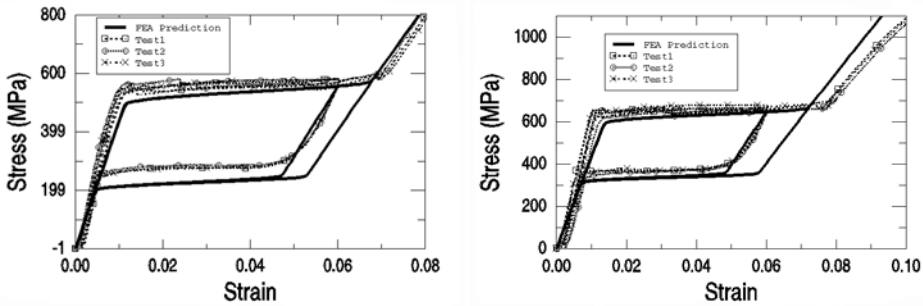


Figure 3 (left) Comparison of the uniaxial tensile tests on $A_f = 14^\circ\text{C}$ wires with FEA prediction from the $A_f = 27^\circ\text{C}$ input data, (right) Comparison of the uniaxial tensile tests on $A_f = -10^\circ\text{C}$ wires with FEA prediction from the $A_f = 27^\circ\text{C}$ input data.

between the different A_f wires. This is because the deformation is bending dominant and the wire is so well confined in the needle—despite the different material responses for the different A_f temperatures, the strain field is independent of the material response. Figure 5 plots the comparison of strain distributions for different A_f wires and the theoretical prediction based on nonlinear beam theory when the loading portion of the Nitinol's stress-strain response is approximated as piecewise linear elasticity. The results are almost identical. Notice these are the strain distributions in the body portion of the arc of the wire; at the locations where the wire changes from straight to arc the strain is slightly higher. This phenomenon, normally referred to as an end effect, can only be predicted from the FEA. Figure 5 shows the strain distribution at this location with comparison to theoretical prediction. As one can see, the strain is higher than the body portion of the curved wire. Therefore, even theory and FEA agree closely on predicting the strain in the body portion of the curved wire. FEA can also capture the end effect nicely and predict the strain more accurately.

This analysis technique also applies to other wire-shaped devices such as a duct-occlusion device, a radio frequency interstitial tissue ablation device, and a hingeless grasper [1–2] and withdrawing of a vena cava filter.

STENT FATIGUE ANALYSIS

A stent is a metal mesh made either from fine wires or from laser cutting tubes into desired patterns set in place to hold a vessel open. The superelastic behavior of Nitinol eased the design due to its large strain capability. Duerig et al. discussed the most important differences between a balloon expandable stent normally made of stainless steel and a self-expanding stent made of Nitinol in addition to the key design issues [21–22]. Regardless of their differences, the most important design issues for a successful stent remain its fatigue life and the stent stiffness. Testing of a Nitinol stent's stiffness and corresponding prediction from nonlinear FEA was straightforward. Gong et al. have demonstrated recently that FEA prediction of a Nitinol's stiffness agrees with the experiment [16].

However, prediction of a Nitinol stent's fatigue performance was not an easy task. Based on the fundamental strain-life approach, prediction of a stent's fatigue performance required a precise analysis of the fatigue strains of a stent *in vivo* and a profound understanding of Nitinol's fatigue behavior under the similar deformation patterns. Nonlinear FEA has been shown to be very effective in computing the fatigue stresses of a balloon expandable stent made of stainless steel

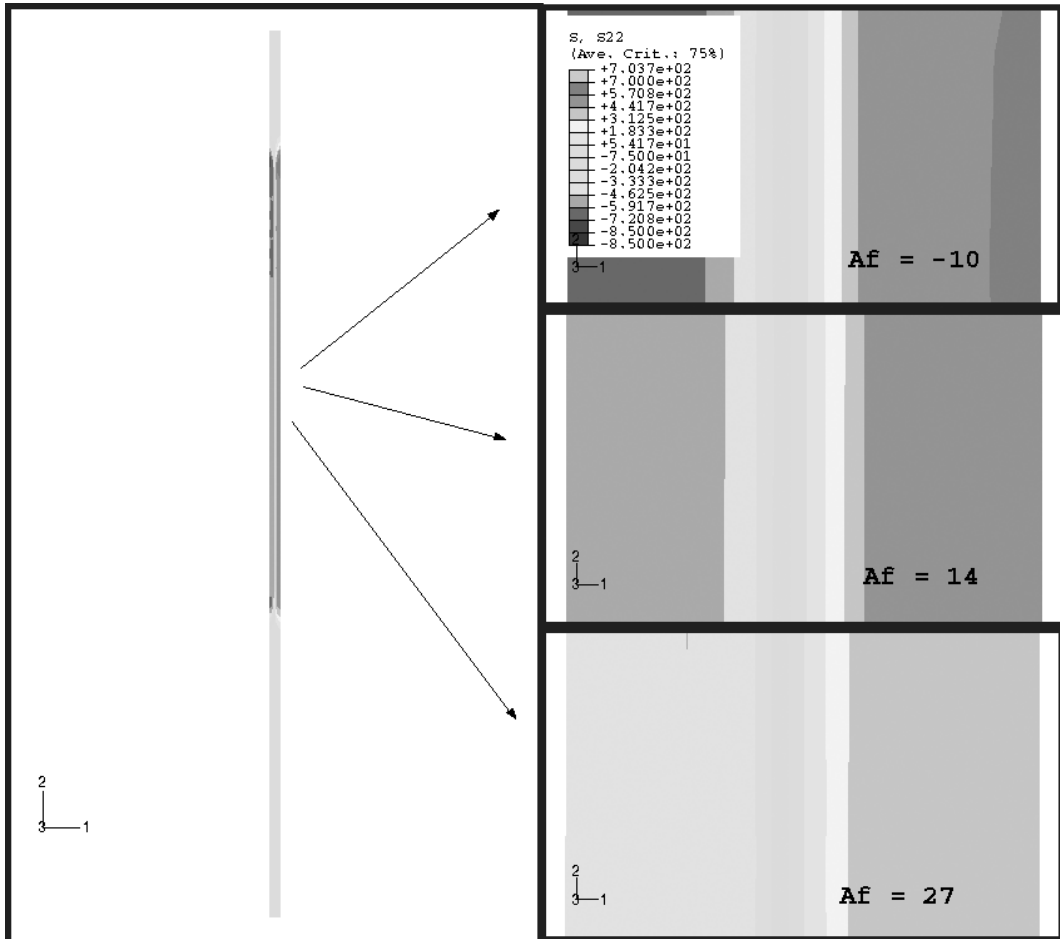


Figure 4 Longitudinal stress contours in the same scale when a different A_f Nitinol locator has been withdrawn inside the needle indicates stress increases as A_f decreases.

[23]. A similar approach applies to Nitinol self-expanding stents, yet Nitinol's complicated material properties and multiple expansion and shape set steps in stent manufacturing discouraged the fatigue analysis of the self-expanding stent's fatigue strains in a single FEA from the "as-cut" stent configuration. Therefore, we proposed to compute the Nitinol self-expanding stent's fatigue strain from its manufactured configuration. An example of an FEA model for computing the fatigue strains of a Nitinol stent *in vivo* is shown in Figure 6. The model contained a Nitinol stent and a straight artery to simulate the interaction of a stent and the artery *in vivo*. Because the fundamental fatigue data or the strain-life curve was collected on the loading portion of Nitinol's stress-strain response, it was very important that the fatigue strain was also evaluated on the loading portion of Nitinol's stress-strain response. For this reason, the fatigue strain analysis technique for a Nitinol self-expanding stent was simulated in the following two steps. The flexible contact between the artery and the stent was "turned off" until the final stage of the analysis. To ensure that the fatigue strains are evaluated at the loading path of the Nitinol, the first step of analysis was to expand the artery to a diameter that was slightly larger than the stent outer diameter (OD). This was done by

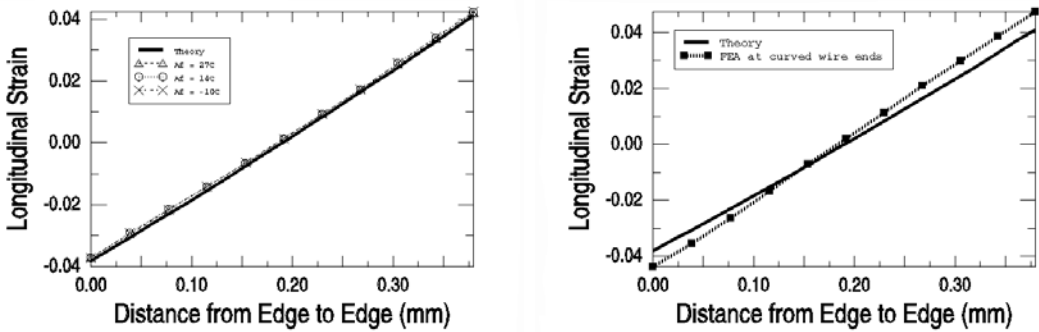


Figure 5 (left) Edge-to-edge longitudinal strain distribution when Nitinol locator was withdrawn inside the needle, (right) Edge-to-edge longitudinal strain distribution comparison at the end of a curved wire when it was withdrawn inside the needle.

applying an internal pressure on the artery. In the second step, the contact between artery and stent was turned on and the pressure applied to the artery in the first step was now ramped down to zero. As the pressure was ramped down, the artery diameter reduced and therefore the interaction between the stent and the artery occurred when the contact between stent OD and the artery surface was established. This portion of analysis placed strain on the stent as a function of the pressure on the stented artery. Fatigue strains were then determined by locating the strains at different pressures. Clearly the alternating strain was dependent upon the vessel compliance and the pressure differential. The mean strain, on the other hand, was dominant by the amount of oversizing. Our calculation indicated that the Cordis-NDC SMARTTM family of stents had a mean strain from 1% to 2% per their product IFU.

In addition to fatigue strains, one can also obtain the stent diameters at different pressures. In our studies on several Nitinol self-expanding stent product lines, FEA predictions of stent diameters agreed extremely well with the actual lab measurement of the stent diameters. These built confidence on the fatigue strain predictions [24].

To establish a fatigue baseline (a strain-life curve) for stent application, the test specimen must have similar deformation patterns to the deformation of a stent *in vivo*. A direct and efficient way to establish the strain-life curve for a stent is to perform fatigue testing on its individual struts. However, such “unzipped stents” are not easy to handle experimentally. We therefore built a unit cell of a stent, i.e., a diamond shaped specimen, to overcome the handling difficulties (Figure 7). It was designed to be similar to the strut geometry from several commercially available stents. The small holes in the ends of the sample were to assist in alignment and gripping the sample. The samples were processed in the same manner as a stent so that it had the same A_f and electropolished surface finish. They were stretched and compressed before the actual fatigue test and the load and displacement were recorded to ensure the processing consistency in sample preparation [22].

FEA was used to calculate the strain field in the specimen so that the test could be planned at the most relevant *in vivo* conditions for stent application; the results were interpreted as a strain-life curve [22]. Notice that when only the loading portion of the curve was considered, one could simplify the stress-strain curve as piecewise linear. Under this simplification, the beam theory was used to estimate the maximum strain inside the specimen and predict the load-displacement relation on

the loading path to confirm the FEA. Figure 8 shows that the theoretical prediction, FEA, and the experimental data agreed closely.

Fatigue tests were performed during the past two years and the test results were presented in reference [17]. By using the same analysis code and controlling the same process procedures, we were able to ensure fatigue safety. Accelerated device tests performed on several stent product lines have confirmed our predictions.

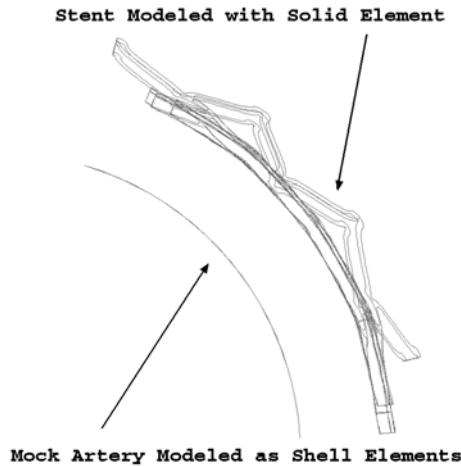


Figure 6 FEA model for stent fatigue strain analysis includes multiple rows of struts to cover the end effects and an artery to simulate the stent-artery interaction.



Figure 7 Diamond shaped specimen for fatigue study.

CONCLUSION

From two typical minimally invasive medical device applications, we showed that nonlinear FEA has opened the door for Nitinol engineering evaluations. This indicates it can be used as a predictive tool prior to prototyping the designs to optimize the device functionality, not only by varying the geometry of the design, but also by tuning the material properties. In addition, FEA can identify the fatigue strains at given *in vivo* conditions. This approach also addresses the device's fatigue life, which is essential for most implantable devices, provided a strain-life curve has been established from the same FEA to ensure consistency. To summarize, the use of FEA helps one to understand the device functionality and the fatigue properties of Nitinol. Experiments coupled with FEA can guide the device designer in improving service life and optimizing the device functionality.

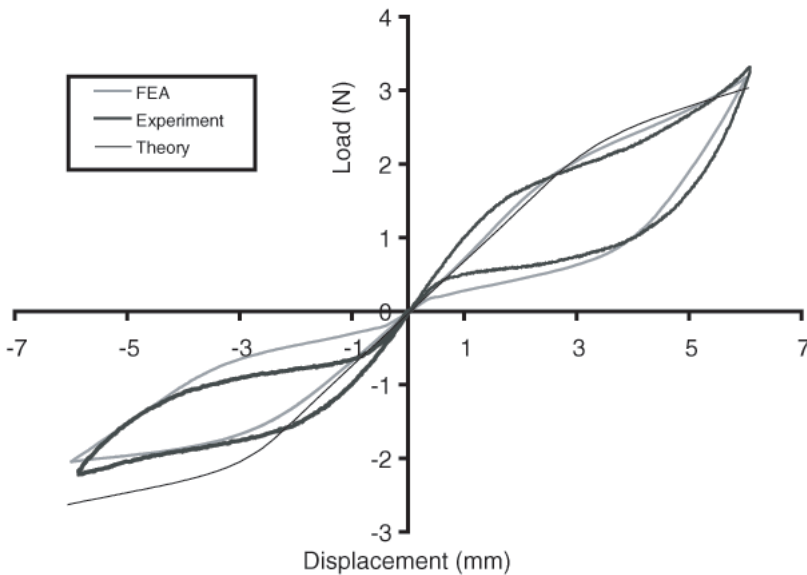


Figure 8 Comparison of FEA, theoretical prediction, and experimental data of load-displacement relation on a diamond-shaped specimen.

REFERENCES

1. D. Stoeckel, *Min, Invas. Ther. & Allied Technologies* **9** No. 2 (2000), p. 81.
2. D. Stoeckel and A. Melzer, *Materials in Clinical Applications*, eds. Vincenzini, P. and Techna Srl (1995), p. 791.
3. S. Miyazaki in *Shape Memory Materials*, eds. K. Otsuka and C.M. Wayman (Cambridge University Press, 1999), p. 267.
4. NDC web site, www.nitinol.com.
5. D. Tolomeo, T. Slater, and P. Wu in *SMST-2000: Proceedings of the International Conference on Shape Memory and Superelastic Technologies*, eds. S.M. Russell and A.R. Pelton (Pacific Grove, Calif.: International Organization on SMST, 2000), p. 517.
6. L. Anand and M. Kothari, *J. Mech. Phys. Solids* **44** (1996), p. 525.
7. F. Auricchio and R.L. Taylor, *Comput. Methods Appl. Mech. Engrg.* **143** (1996), p. 175–194.
8. F. Auricchio, R.L. Taylor, and J. Lubliner, *Comput. Methods Appl. Mech. Engrg.* **146** (1997), p. 281.
9. M.A. Qidwai and D.C. Lagoudas, *Int. J. Numer. Meth. Engng.* **46** (2000), p. 1123.
10. J. Knowles, *Comput. Mech.* **22** (1999), p. 429.
11. E. Patoor, A. Eberhardt, and M. Berveiller, *J. Phys.* **IV 6** (1996), p. 277.

12. Q. Sun and K. Hwang, *J. Mech. Phys. Solids* **41** (1993), p. 1.
13. Q. Sun and K. Hwang, *J. Mech. Phys. Solids*, **41** (1993).
14. N. Rebelo and M. Perry, *Min. Invas. Ther. & Allied. Technol.* **9** (2) (2000), p. 75.
15. N. Rebelo, M. Hsu and H. Foadian in *SMST-2000: Proceedings of the International Conference on Shape Memory and Superelastic Technologies*, eds. S.M. Russell and A.R. Pelton (Pacific Grove, Calif.: International Organization on SMST, 2000), p. 495.
16. X.-Y. Gong, A.R. Pelton, T.W. Duerig, N. Rebelo, and K.E. Perry in *SMST 2003: Proceedings of the International Conference on Shape Memory and Superelastic Technologies*, eds. A.R. Pelton and T. Duerig (Pacific Grove, Calif: International Organization on SMST, in press).
17. X.-Y. Gong, A.R. Pelton, and T.W. Duerig in *SMST 2003: Proceedings of the International Conference on Shape Memory and Superelastic Technologies*, eds. A.R. Pelton and T. Duerig (Pacific Grove, Calif: International Organization on SMST, in press).
18. J.P. O'Leary, J.E., Nicholson, and R.F. Gattorna in *Engineering Aspects of Shape Memory Alloys*, eds. T.W. Duerig, K.N. Melton, D. Stoeckel, and C.M. Wayman (1990), p. 477.
19. A.R. Pelton, J. Dicello and S. Miyazaki, *Min. Invas. Ther. & Allied. Technol.* **9** (2) (2000), p. 107.
20. A.R. Pelton, T.W. Duerig, and D. Stoeckel, *Designing with Nitinol* (Presented at SMST 2001, in Kunming, China, Sept. 2001).
21. T.W. Duerig and M. Wholey, *Min. Invas. Ther. & Allied. Technol.* **11** (4) (2002), p. 173.
22. T. Duerig, D.E. Tolomeo, and M. Wholey, *Min. Invas. Ther. & Allied. Technol.* **9** (3/4) (2000), p. 235.
23. S. Oh in *ABAQUS Users' Conference Proceedings* (Newport, R.I., June 2000), p. 535.
24. X.-Y. Gong, L. Zhu and A.R. Pelton (unpublished work).